

## keV Neutron Capture Cross Section of $^{170}\text{Yb}$

B. J. Allen<sup>A</sup> and D. D. Cohen<sup>B</sup>

<sup>A</sup> AAEC Research Establishment, Private Mail Bag, Sutherland, N.S.W. 2232.

<sup>B</sup> Australian Institute of Nuclear Science and Engineering, AAEC Research Establishment, Private Mail Bag, Sutherland, N.S.W. 2232.

### Abstract

The neutron capture cross section of  $^{170}\text{Yb}$  has been measured relative to gold in the neutron energy range 10-70 keV. The 30 keV average cross section is  $790 \pm 60$  mb. The astrophysical significance of this result is discussed with respect to the  $^{176}\text{Lu}$ - $^{176}\text{Hf}$  cosmochronometer.

### Introduction

The isotope  $^{170}\text{Yb}$  is of particular interest in astrophysics because it is formed solely by the s process of nucleosynthesis (Burbidge *et al.* 1957). Its neutron capture cross section  $\langle\sigma\rangle$  at temperatures similar to those of stellar interiors can provide an improved estimate of the magnitude of the s-process parameter  $(N_s\langle\sigma\rangle)_A$  (where  $N_s$  is the s-process abundance) in the  $140 < A < 190$  mass region and can lead to a more accurate estimate of the mean age of s-process nucleosynthesis (McCulloch *et al.* 1976). The neutron capture cross section of  $^{170}\text{Yb}$  is also required to complement the recent measurements of Shorin *et al.* (1975) on the heavier ytterbium isotopes, and so provide further information on systematic odd-even neutron number effects in these nuclides.

### Measurements

The AAEC 3 MeV Van de Graaff accelerator was used with terminal pulsing and bunching to produce a 1 MHz pulsed proton beam. The  $^7\text{Li}(p, n)$  reaction supplied the neutron source, with the incident proton energy being 12 keV above the threshold energy. Neutrons were produced in an energy range 7-75 keV within a forward cone of  $35^\circ$  half angle.

Targets of 10 cm diameter were placed at a flight path of 30 cm from the neutron source, and capture  $\gamma$  rays were observed by a pair of Moxon-Rae detectors (Moxon and Rae 1963), using C-Bi converters (Fig. 1). The Moxon-Rae detectors were surrounded by 5 cm thick lead shielding, and were placed at a back angle ( $\sim 126^\circ$ ) for viewing the capture  $\gamma$  rays, so as to minimize  $\gamma$ -ray attenuation in the target. Since the second-order Legendre polynomial is zero at  $125^\circ$ , the back-angle position reduces the dependence of the capture yield on the  $\gamma$ -ray angular distributions. The high multiplicities of the gold and ytterbium  $\gamma$ -ray spectra also tend to diminish angular effects. The detectors were placed at a half angle to the beam of  $35^\circ$  so that they were clear of the neutron cone for a proton energy of 12 keV above the threshold. A  $^6\text{Li}$  glass scintillator (1 mm thick) monitored the transmitted neutron beam and allowed all runs to be normalized to the same incident neutron flux.

Measurements were made at  $\sim 3$  min intervals on targets of a  $\text{Yb}_2\text{O}_3$  sample (packed in a magnesium can), a carbon sample, a 'no sample' and a gold sample. The targets were cycled by computer control for a preset integrated proton charge (Stroud 1972). In this way, any variations in the incident neutron flux resulting from instability in the proton energy and from lithium target contamination were averaged out. The target diameter  $D$ , mass  $M$ , atom density per barn  $n_A$ ,  $\gamma$ -ray attenuation coefficient  $C_\gamma$ , neutron self-shielding coefficient  $C_s$  and neutron multiple scattering coefficient  $C_M$  are listed for each of the target samples in Table 1.

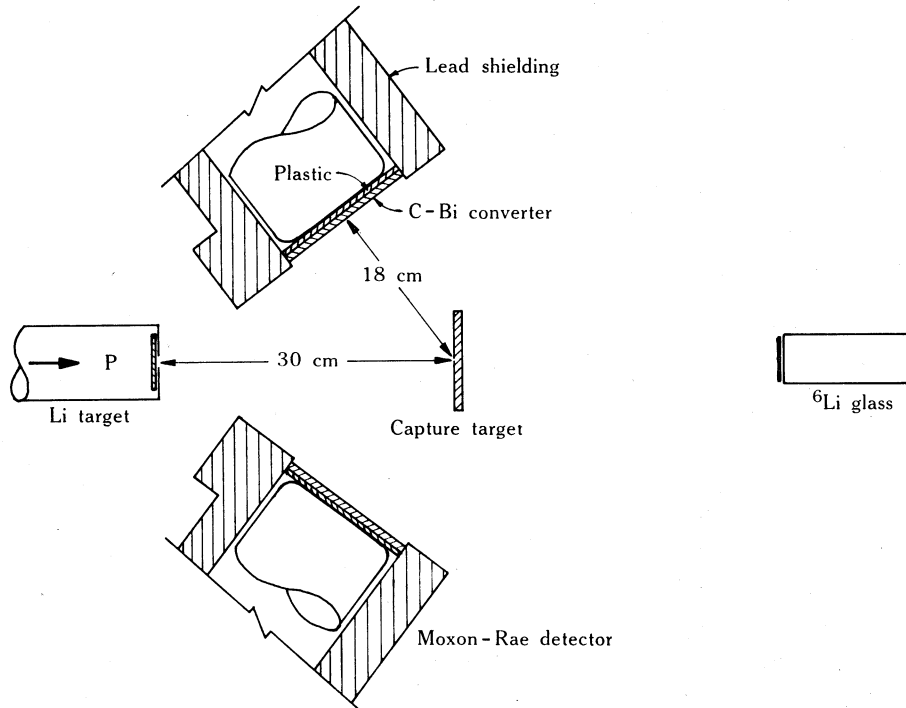
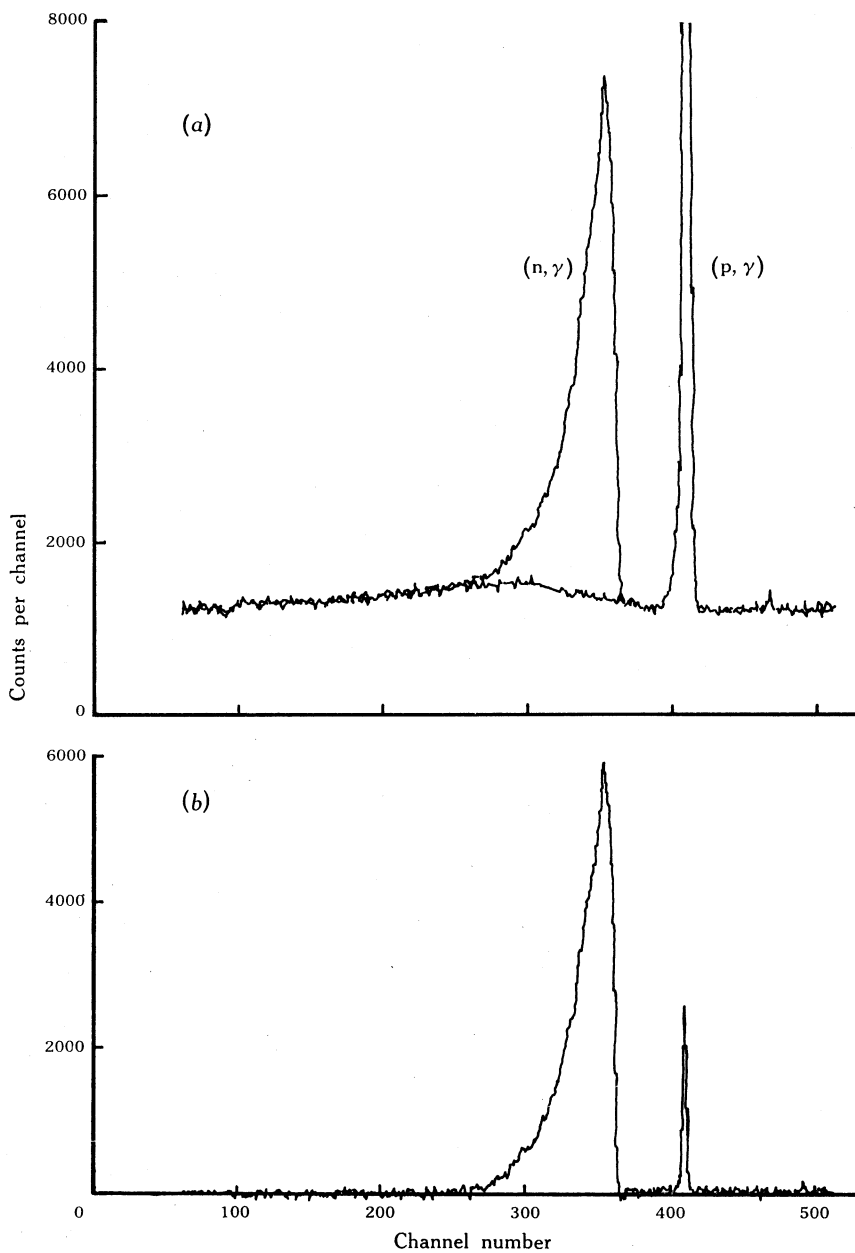


Fig. 1. Schematic diagram of the neutron capture experiment.

Table 1. Data for neutron capture targets

	$D$ (cm)	$M$ (g)	$n_A$ (at. b $^{-1}$ )	$C_\gamma$	$C_s$	$C_M$
$\text{Yb}_2\text{O}_3$	10.0	52.68	0.00208	0.98	0.97	0.020
Mg	11.2	36.72	0.0078			
C	10.0	32.21	0.0206	—	—	—
Au	10.0	78.47	0.00305	0.97	0.98	0.04

Constant fraction timing was employed for the Moxon-Rae and  $^6\text{Li}$  glass detectors to achieve a timing resolution of 3.3 ns (FWHM) for the  $(p, p'\gamma)$  and  $(p, \gamma)$  events of  $^7\text{Li}$ . The Moxon-Rae time of flight events were gated to eliminate low pulse height events, improving the capture-to-background ratio and reducing the effect of sample-scattered neutrons. A pulse height window was also set on the  $^6\text{Li}(n, \alpha)\text{T}$  events to eliminate the  $\gamma$ -ray background. Time of flight Moxon-Rae spectra for the ytterbium and carbon samples are shown in Fig. 2a.



**Fig. 2.** Time of flight spectra for neutron capture in  $^{170}\text{Yb}$ : (a) the sample yield (upper curve) together with the carbon-scattered background (lower curve) and (b) the net sample yield obtained by subtracting out the carbon-scattered background. Zero time occurs at the (p,  $\gamma$ ) peak, and the neutron time of flight scale (1 ns per channel) increases with decreasing channel number.

## Analysis

After normalization for equal incident neutron fluxes, the  $\gamma$ -ray yield for the 'no sample' measurement was subtracted from the yields for the  $\text{Yb}_2\text{O}_3$ , carbon and gold samples. This effectively removed most of the time-independent background as well as the  $(p, \gamma)$  and  $(p, p'\gamma)$  events of  ${}^7\text{Li}$  at zero time of flight. The scattered neutron background was then removed from the  $\text{Yb}_2\text{O}_3$  and gold spectra after normalizing the carbon spectrum for equal scattering to the  $\text{Yb}_2\text{O}_3$  and gold targets in each case. The net capture  $\gamma$ -ray yield for the  $\text{Yb}_2\text{O}_3$  sample is shown in Fig. 2*b*.

**Table 2. Comparison of neutron capture data for  ${}^{197}\text{Au}$ ,  ${}^{171}\text{Yb}$  and  ${}^{170}\text{Yb}$**

The mean standard deviation for  $Y_{\text{Yb}}/Y_{\text{Au}}$  is 1.8%, for  $\langle\sigma_{197}\rangle$  is  $\leq 4.0\%$ , for  $\langle\sigma_{171}\rangle$  is 8.4% and for  $\langle\sigma_{170}\rangle$  is 8.6%

Energy range (keV)	$Y_{\text{Yb}}/Y_{\text{Au}}$	$\langle\sigma_{197}\rangle^{\text{A}}$ (mb)	$\langle\sigma_{171}\rangle^{\text{B}}$ (mb)	$\langle\sigma_{170}\rangle^{\text{C}}$ (mb)
10-15	$0.939 \pm 0.035$	1011	2253	$1208 \pm 122$
15-20	$0.970 \pm 0.023$	778	1817	$941 \pm 84$
20-30	$1.075 \pm 0.014$	621	1560	$855 \pm 69$
30-40	$1.077 \pm 0.012$	529	1336	$728 \pm 58$
40-50	$1.105 \pm 0.011$	453	1207	$625 \pm 51$
50-60	$1.149 \pm 0.014$	423	1113	$634 \pm 50$
60-70	$1.235 \pm 0.029$	384	989	$650 \pm 51$
20-40		575	1448	$792 \pm 63$

<sup>A</sup> Measurements from Macklin *et al.* (1975); <sup>B</sup> measurements from Shorin *et al.* (1975); <sup>C</sup> present measurements.

**Table 3. Data for calculating isotopic  $\gamma$ -ray yields**

Isotope	$f_A$ (%)	$E_b$ (MeV)	$\langle\sigma_A\rangle_{30}$ (mb)	$E_r$ (keV)	$A_\gamma$ (b eV)	$Y_A$ (MeV mb)
${}^{168}\text{Yb}$	0.03	6.89	$(1500) \pm 300^{\text{A}}$			3.1
${}^{170}\text{Yb}$	68.5	6.65				$4.555 \langle\sigma\rangle$
${}^{171}\text{Yb}$	15.9	8.24	$1438 \pm 120^{\text{B}}$			1838
${}^{172}\text{Yb}$	7.75	6.38	$402 \pm 33^{\text{B}}$			198.8
${}^{173}\text{Yb}$	2.86	7.50	$885 \pm 75^{\text{B}}$			189.8
${}^{174}\text{Yb}$	3.90	5.85	$183 \pm 16^{\text{B}}$			41.8
${}^{176}\text{Yb}$	1.05	5.60	$110 \pm 11^{\text{B}}$			6.5
${}^{197}\text{Au}$	100	6.51	$579 \pm 8^{\text{C}}$			3905
${}^{24}\text{Mg}$	78.99	7.33		4.64	86	
${}^{25}\text{Mg}$	10.0	11.1		{ 19.0	160	
${}^{26}\text{Mg}$	11.0	6.43		{ 62.9	94	
				68.7	48	

<sup>A</sup> Estimated value; <sup>B</sup> measurement from Shorin *et al.* (1975); <sup>C</sup> measurement from Macklin *et al.* (1975).

The ratio  $Y_{\text{Yb}}/Y_{\text{Au}}$  of the net  $\gamma$ -ray yields for the  $\text{Yb}_2\text{O}_3$  and gold samples (corrected for target effects) was obtained for the energy bins given in Table 2, and is seen to be energy dependent. The energy-integrated ratio (from 7 to 70 keV) was found to be  $1.15 \pm 0.02$ , where the standard deviation is statistical only. Two separate measurements of this quantity agreed within the errors. Table 2 also compares experimental

data for the average neutron capture cross sections (within the same energy bins) for  $^{197}\text{Au}$  (Macklin *et al.* 1975),  $^{171}\text{Yb}$  (Shorin *et al.* 1975) and  $^{170}\text{Yb}$  (present results). In addition, 30 keV values  $\langle\sigma\rangle_{30}$  are given, these being means over 20–40 keV.

The important property of the Moxon–Rae detector is the linear dependence of its efficiency on the incident  $\gamma$ -ray energy. Thus the detector efficiency (for single events) is proportional to the total energy (i.e. binding energy plus centre of mass neutron energy) of the capture reaction, and independent of the details of the  $\gamma$ -ray spectrum.

For the  $\text{Yb}_2\text{O}_3$  sample, capture yields occur for each isotope and also for the magnesium container. Isotopic abundances  $f_A$ , binding energies  $E_b$  and average capture cross sections  $\langle\sigma\rangle_{30}$  at 30 keV are given in Table 3 for the isotopes of ytterbium, gold and magnesium. In addition, resonance energies  $E_r$  and  $\gamma$ -ray capture areas  $A_\gamma$  from Weigmann *et al.* (1976) are given for the magnesium isotopes.

The observed  $\gamma$ -ray yield  $Y_\gamma$  per incident neutron per  $\text{cm}^2$  at 30 keV for the  $\text{Yb}_2\text{O}_3$  target is given by the sum of the capture yields of its constituents, each of which is proportional to the product of the number of atoms per unit area, the average capture cross section and the total energy of the capture reaction. Thus we have

$$Y_\gamma = k \sum_A n_A \langle\sigma_A\rangle_{30} E_A^T, \quad (1)$$

where  $n_A$  is the atom density per barn for mass number  $A$ ,  $k$  is a constant and  $E_A^T$  is the total energy for the capture reaction. For the ytterbium sample we sum the relative isotopic yields

$$Y_A = E_A^T \langle\sigma_A\rangle_{30} f_A, \quad (2)$$

which are given in Table 3, normalizing to the thickness ( $\text{at. b}^{-1}$ ) of the natural ytterbium target, to obtain

$$Y_{\text{Yb}} = 0.00208 k (4.555 \langle\sigma_{170}\rangle_{30} + 2277) C_\gamma (C_S + C_M). \quad (3)$$

The  $\gamma$ -ray attenuation  $C_\gamma$  and the neutron self-shielding and multiple scattering corrections  $C_S + C_M$  are close to unity, and are given in Table 1. The neutron corrections were obtained by Monte Carlo methods (Sullivan *et al.* 1969). This relation holds only at 30 keV since the energy dependence of the major ytterbium isotopic contaminant ( $^{171}\text{Yb}$ ) is dissimilar to that of gold. Calculations are therefore needed for each energy bin using the capture cross section for  $^{171}\text{Yb}$  taken from Shorin *et al.* (1975) and given in Table 2. An additional correction for magnesium capture is required at other energies (see Table 3).

The standard gold cross section was taken from Macklin *et al.* (1975) and is given in Table 2, averaged over the energy bins. Macklin *et al.* obtained a fitted curve average at 30 keV of  $579 \pm 8$  mb, which is in excellent agreement with the 30 keV value by Czirr and Stelts (1975) of  $585 \pm 17$  mb. The standard cross section is also in good agreement (to better than 4%) with the evaluation by Poenitz (1971). Although the accuracy of the standard gold cross section is estimated at 1.4%, a value of 4% was adopted, which adequately covers the Poenitz evaluation as well.

The statistical error for the determination of the capture yield ratio is typically (1–2)% for each energy bin, increasing at the lower and upper energies where the neutron flux drops off. A major source of error arises from the contribution of the

heavier ytterbium isotopes to the capture yield. From Table 3 it is apparent that the major correction occurs for  $^{171}\text{Yb}$ , for which Shorin *et al.* (1975) quoted an error of  $\sim 8.3\%$  for the cross section of this isotope. These errors contribute to a final average standard deviation of  $8.6\%$  for the energy-bin-averaged capture cross section of  $^{170}\text{Yb}$ .

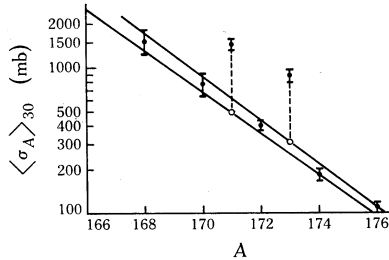


Fig. 3. Semi-empirical determination of the 30 keV capture cross sections  $\langle\sigma_A\rangle_{30}$  of  $^{168}\text{Yb}$  and  $^{170}\text{Yb}$ . The average ratio of the odd-mass cross sections to the interpolated values from the even-mass isotopes is  $2.9 \pm 0.3$ .

Table 4. Average 30 keV capture cross sections for the isotopes of ytterbium

Values given in parentheses used for normalization; errors are one standard deviation

Source of data	$\langle\sigma_{168}\rangle_{30}$ (mb)	$\langle\sigma_{170}\rangle_{30}$ (mb)	$\langle\sigma_{171}\rangle_{30}$ (mb)	$\langle\sigma_{172}\rangle_{30}$ (mb)	$\langle\sigma_{173}\rangle_{30}$ (mb)	$\langle\sigma_{174}\rangle_{30}$ (mb)	$\langle\sigma_{176}\rangle_{30}$ (mb)
(a) Experimental results							
Shorin <i>et al.</i> (1975)			$1438 \pm 120$	$402 \pm 33$	$885 \pm 75$	$183 \pm 16$	$110 \pm 11$
Present work		$792 \pm 63$					
Stupegia <i>et al.</i> (1968)							$200 \pm 30$
(b) Theoretical results							
Benzi <i>et al.</i> (1972)	690	1060	1200	630	990	250	210
Allen <i>et al.</i> (1971)	700	510	1320	380	990	275	(200)
Holmes <i>et al.</i> (1976)	1110	990	1510	534	1130	190	183
Present work	$1500 \pm 300$	$770 \pm 150$	(1438)	(402)	(885)	(183)	(110)

### Comparison with Estimated Cross Sections

Calculated capture cross sections from Allen *et al.* (1971), Benzi *et al.* (1972) and Holmes *et al.* (1976) are given in Table 4, together with new semi-empirical estimates based on the isotopic cross sections of Shorin *et al.* (1975). These new values supersede those of Allen *et al.* (1971), which were based on the only cross section (that for  $^{176}\text{Yb}$ ) which had been measured at that time. The semi-empirical estimates are derived as follows. An exponential interpolation from the even- $A$  isotopes provides cross sections for each odd isotope which may be compared with the measured values. The ratio of measured and even- $A$  interpolated cross sections for  $^{171}\text{Yb}$  and  $^{173}\text{Yb}$  is found to be constant to 10%, namely  $2.9 \pm 0.3$  (see Fig. 3). An exponential extrapolation to  $^{170}\text{Yb}$  from the even- $A$  cross sections can therefore be reliably made to obtain a value of  $770 \pm 150$  mb for  $^{170}\text{Yb}$  and  $1500 \pm 300$  mb for  $^{168}\text{Yb}$ . This semi-empirical method for estimating capture cross sections was shown by Allen *et al.* (1971) to be widely applicable. The  $^{170}\text{Yb}$  cross section is in excellent agreement with our measured value of  $792 \pm 63$  mb, while Hauser-Feshbach calculations by Benzi *et al.* (1972) and Holmes *et al.* (1976) are high by 40% and 30% of the experimental value respectively. Predictions for  $^{168}\text{Yb}$  vary by a factor of more than two, but are unlikely to be experimentally tested because of the low abundance of this isotope.

### Astrophysical Implications

The s-process parameter  $(N_S \langle \sigma \rangle)_A$  in the region of lutetium can now be accurately evaluated, using the solar system abundance for  $^{170}\text{Yb}$  of  $N_S = 0.0067$  (relative to silicon =  $10^6$  at.) determined by McCulloch *et al.* (1976). The new value at 30 keV is  $(N_S \langle \sigma \rangle)_{170} = 5.3$ , which lies between the results for the samarium (6.8 and 6.3) and osmium (3.5 and 3.7) s-process isotopes, and confirms the predicted mass dependence for  $(N_S \langle \sigma \rangle)_A$  in the  $140 < A < 190$  mass region (Allen *et al.* 1971).

The mean duration of s-process nucleosynthesis ( $\Delta$  years) can be estimated using the Schramm–Wasserburg (1970) formalism:

$$\Delta = \lambda_{176}^{-1} \ln(B(N_S \langle \sigma \rangle)_{170} / (N_S \langle \sigma \rangle)_{176}), \quad (4)$$

where  $B$  is the branching ratio to the ground state for the reaction  $^{175}\text{Lu}(n, \gamma)^{176}\text{Lu}$  at 30 keV, which decays with a half-life of  $3.6 \times 10^{10}$  yr, and  $\lambda_{176} = 1.93 \times 10^{-11}$  s. The branching ratio is estimated to be  $B = 0.33 \pm 0.17$  (Audouze *et al.* 1972).

The cosmic abundance of  $^{176}\text{Lu}$  (at the condensation of the solar system) was given by McCulloch *et al.* (1976) as 0.00097, and Macklin and Gibbons (1967*a*, 1967*b*) obtained a value of  $2246 \pm 170$  mb for the 30 keV capture cross section of  $^{176}\text{Lu}(n, \gamma)$ . Substituting these values into the above equation yields a negative value for  $\Delta$ . Since all other parameters are well defined, the estimated value for the 30 keV branching ratio would appear to be in error. An accurate measurement of the  $^{176}\text{Lu}$  branching ratio at 30 keV is therefore required before the  $^{176}\text{Lu}$ – $^{176}\text{Hf}$  chronometer can be evaluated.

### Acknowledgments

We are grateful to the U.S. Department of Energy for supplying the enriched sample of  $^{170}\text{Yb}_2\text{O}_3$ . The technical assistance of H. Broe and J. Fallon with the 3 MeV Van de Graaff accelerator is acknowledged, as is the contribution of R. J. Cawley to the on-line computer focal system. We have benefited from discussions with J. R. de Laeter who suggested this experiment.

### References

- Allen, B. J., Gibbons, J. H., and Macklin, R. L. (1971). *Adv. Nucl. Phys.* **4**, 205.  
 Audouze, J., Fowler, W. A., and Schramm, D. N. (1972). *Nature Phys. Sci.* **283**, 8.  
 Benzi, V., d'Orazi, R., de Reffo, G., and Vaccari, M. (1972). Comitato Nazionale Energia Nucleare Rep. No. RT/F172(6).  
 Burbidge, E. N., Burbidge, G. R., Fowler, W. A., and Hoyle, F. (1957). *Rev. Mod. Phys.* **29**, 547.  
 Czirr, J. B., and Stelts, M. L. (1975). *Nucl. Sci. Eng.* **52**, 299.  
 Holmes, J. A., Woosley, S. E., Fowler, W. A., and Zimmerman, B. A. (1976). *At. Data Nucl. Data Tables* **18**, 305.  
 McCulloch, M. T., de Laeter, J. R., and Rosman, K. J. R. (1976). *Earth Planet Sci. Lett.* **28**, 308.  
 Macklin, R. L., and Gibbons, J. H. (1967*a*). *Astrophys. J.* **149**, 577.  
 Macklin, R. L., and Gibbons, J. H. (1967*b*). *Phys. Rev.* **159**, 1007.  
 Macklin, R. L., Halperin, J., and Winters, R. R. (1975). *Phys. Rev. C* **11**, 1270.  
 Moxon, M. C., and Rae, E. R. (1963). *Nucl. Instrum. Methods* **24**, 445.  
 Poenitz, W. P. (1971). A.E.C. Symp. Ser. Rep. No. 23 (Aug.).  
 Schramm, D. N., and Wasserburg, G. J. (1970). *Astrophys. J.* **162**, 57.  
 Shorin, V. S., Kononov, V. M., and Poletaev, E. D. (1975). *Sov. J. Nucl. Phys.* **20**, 572.

- Stroud, D. B. (1972). Ph.D. Thesis, University of Melbourne.
- Stupegia, D. C., Schmidt, M., Keedy, C. R., and Madson, A. A. (1968). *J. Nucl. Energy* **22**, 267.
- Sullivan, J. G., Warner, G. G., Block, R. C., and Hockenbury, R. W. (1969). Rensselaer Polytechnic Institute Rep. No. 328-155.
- Weigmann, H., Macklin, R. L., and Harvey, J. A. (1976). *Phys. Rev. C* **14**, 1328.

Manuscript received 8 January 1979